AKENTEN APPIAH MENKA UNIVERSITY OF SKILLS AND ENTREPRENEURIAL DEVELOPMENT, KUMASI.

THE EFFECTS OF WELDING PARAMETERS ON THE MECHANICAL PROPERTIES ON MANUAL METAL ARC WELDING OF A36 LOW CARBON STEEL.

BEDIAKO BANABAS NYANTAKYI

(7211220002)

2023

AKENTEN APPIAH MENKA UNIVERSITY OF SKILLS AND ENTREPRENEURIAL DEVELOPMENT, KUMASI.

THE EFFECTS OF WELDING PARAMETERS ON THE MECHANICAL PROPERTIES ON MANUAL METAL ARC WELDING OF A36 LOW CARBON STEEL.

BEDIAKO BANABAS NYANTAKYI

(7211220002)

A DISSERTATION SUBMITTED TO THE DEPARTMENT OF MECHANICAL AUTOMOTIVE TECHNOLOGY EDUCATION, FACULTY OF TECHNICAL EDUCATION OF THE SCHOOL OF GRADUATE STUDIES, AKENTEN APPIAH MENKA UNIVERSITY OF SKILLS AND ENTREPRENEURIAL DEVELOPMENT, KUMASI IN PARTIAL FULFILLMENT OF THE REQUIREMENTS FOR THE AWARD OF MASTER OF TECHNOLOGY (MECHANICAL ENGINEERING DEGREE

DECEMBER 2023

DECLARATION

STUDENT'S DECLARATION

I, Bediako Banabas Nyantakyi, declare that this Desertation, with the exception of quotations and references contained in published works which have all been identified and duly acknowledged, is entirely my own original work, and it has not been submitted, either in part or whole, for another degree elsewhere.

SIGNATURE..... **DATE.....**

SUPERVISOR'S DECLARATION

I hereby declare that the preparation and presentation of this work was supervised in accordance with the guidelines for supervision of Thesis as laid down by the University of Akenten Appiah-Menka University of Skilled Training and Entrepreneurial Development.

NAME OF SUPERVISOR: DR. ENOCH A. DUODU

SIGNATURE.....

DATE.....

ACKNOWLEDGEMENT

This work has not been an easy work. It has involved the help of many individuals: Mr. Bismark Addai of Sunyani Technical University who guided me to complete this work, Michael Anto of Kumasi Technical Institute who allowed me to use their welding laboratory to weld all samples. I am therefore grateful to God Almighty for making my dreams come true.

My special thanks go to my supervisor Dr. Enoch A. Duodu, for his patience, corrections, constant guidance and excellent suggestions, which have been very helpful to me in coming with this work.

DEDICATION

This work is dedicated to my children, Oswald Homeda Nyantakyi, Jaden Nyantakyi

TABLE OF CONTENTS

LIST OF FIGURES

LIST OF TABLES

ABSTRACT

In order to obtain properties that fully satisfy the requirements placed on welded structures; the properties of the heat-affected zone have been examined to identify changes in material properties caused by variations in welding parameters and conditions. The high-temperature fusion process during welding results in microstructural and mechanical property changes close to the weld line, in the heat-affected zone, which significantly alters the parent material's mechanical properties. This work prepares a specimen with Butt and LAP joints in order to examine the tensile test, hardness test, and microstructure of the heat-affected zone of 5mm A36 low carbon steel that was welded using a manual metal arc welding procedure. The goal of the experiment was to determine how heat input influenced the hardness, tensile strength, and microstructure of the heat-affected zone.

The investigation's findings show that a considerable increase in hardness with rising temperatures led to a fall in the hardness rating of the heat-affected zone. According to the experiment, the average heat-affected zone hardness is 16.5% greater than the parent metal hardness, while the average heat-affected zone toughness and tensile strength are 18.5% and 6.5 percent lower than the parent material hardness, respectively. The mechanical parameters of the heat-affected zone did not significantly change when the welding speed was changed. Therefore, it is advised that the plate form and ramp, two low bed semi-trial chassis components, be made using the findings of this work.

CHAPTER ONE

INTRODUCTION

1.1 Background of the study

The exclusive method of joining iron and steel by heating and hammering was forging welding, which was practiced by blacksmiths for centuries until the end of the 19th century. Late in the century, arc and oxy-fuel welding emerged as some of the earliest techniques, with electric resistance welding following shortly after. The need for dependable and affordable joining techniques was fueled by World Wars I and II, which led to a rapid advancement in welding technology in the early 1900s. Following the wars, numerous contemporary welding processes were developed, including semi-automatic and automatic procedures like flux core welding, submerged arc welding, and gas metal arc welding, as well as manual techniques like shielded metal arc welding, which is currently one of the most widely, used welding techniques.

Welding is a fabrication or sculpting technique that creates coalescence to combine materials, most commonly thermoplastics or metals. In order to create a strong union, fusion welding often involves melting the work components and adding filler material to create a pool of molten material, or the "weld pool," which cools. Pressure is occasionally applied in addition to heat or only with heat to create the weld. In contrast, brazing and soldering entail melting a substance with a lower melting point between the work pieces to create a bond without actually melting the work pieces. For welding, a wide range of energy sources can be employed. These consist of an electron beam, a gas flame, an electric arc, and a laser. In the second half of the century, advancements in science led to the introduction of laser beam welding, electron beam welding, electromagnetic pulse welding, and friction stir welding. In industrial settings, robotic welding is a typical occurrence, and researchers are always coming up with new welding techniques and expanding their knowledge of weld quality (Ashby, 1970)

Arc welding progressed slowly following the discoveries of the short-pulsed electric arc by Humphry Davy in 1801 and the continuous electric arc by Vasily Petrov in 1802. The concept

of welding in an inert gas atmosphere was first proposed by C. L. Coffin in 1890. However, non-ferrous elements like magnesium and aluminum remained challenging to weld even in the early 1900s because these metals react quickly with air, producing porous, dross-filled welds. Procedures with flux-covered electrodes did not provide contamination protection for the weld region. In the early 1930s, bottled inert gasses were used as a solution to the issue. A few years later, the aerospace industry developed a direct current, gas-shielded welding method for welding magnesium.

Arc welding progressed slowly following the discoveries of the short-pulsed electric arc by Humphry Davy in 1801 and the continuous electric arc by Vasily Petrov in 1802. Although the concept of welding in an inert gas atmosphere was first proposed by C. L. Coffin in 1890, non-ferrous materials like magnesium and aluminum were still challenging to weld due of their fast air reaction. The procedure was refined in 1941 by Northrop Aircraft's Russell Meredith. Though it is frequently referred to as tungsten inert gas welding, Meredith called the procedure Heliarc since it used a tungsten electrode arc and helium as a shielding gas (TIG). Gas tungsten arc welding is the official phrase used by the American Welding Society (GTAW). A variety of water- and air-cooled torch models, gas lenses for enhanced shielding, and other process-enhancing accessories were created by Linde Air Products. Tungsten has a high melting temperature, however at first the electrode overheated rapidly and tungsten particles were transmitted to the weld. The electrode's polarity was switched from positive to negative to solve this issue, but this modification rendered it ineffective for welding a wide range of non-ferrous materials.

Ultimately, the introduction of alternating current units allowed for the stabilization of the arc and the production of excellent magnesium and aluminum welds.

Changes persisted in the decades that followed. In order to help avoid overheating when welding with high currents, Linde invented water-cooled torches. When the process became more popular in the 1950s, some users tried using carbon dioxide instead of the costlier argon

and helium welding atmospheres. However, this did not work well for welding magnesium and aluminum because it resulted in a lower-quality weld, so today; carbon dioxide is hardly ever used in conjunction with gas tungsten arc welding (GTAW). Any shielding gas that contains carbon dioxide or another oxygen compound will quickly contaminate the tungsten electrode and render it unfit for use in the TIG process. Plasma arc welding is a new technique that was created in 1953 and is based on GTAW. While it is mostly restricted to automate equipment, it offers more control and enhances the quality of the weld by focusing the electric arc using a nozzle, while GTAW is still predominantly a manual, hand-held technique. The GTAW process has also undergone continuous development, and there are now several variants. The most widely used GTAW techniques include greater penetration, hot-wire, pulsed-current, hand programmed, and dabber. According to Jeffus (2004), various welding processes are employed in construction machine repair and manufacture (R. P. Singh & Agrawal, 2021a). Certain materials could be able to be welded using one approach, but other materials might not be properly welded using that technique.

The mechanical and weldability characteristics of mild steel are influenced by its chemical makeup. Mild steel is intentionally made with the addition of many components. (Zhao et al., 2014) state that because scrap materials are charged during the steelmaking process, additional undesired elements might also be present. To reduce cracking, higher pre- and post-heating temperatures, improved hydrogen control, and sometimes post-heating are needed. Some elements, such as tungsten, carbon, and manganese, boost strength but also raise the risk. The microstructure of the mild steel weld fusion zone is influenced by the material's chemical makeup and pace of cooling, as per (Brykov et al., 2020). The following formula can be used to determine the critical cooling rate required to achieve mart where V stands for the I kmol/hr critical cooling rate. Heat input, which is affected by welding parameters like welding current and duration, determines the volume of melted metal. As current increases, the fusion zone size decreases, but as time advances, the fusion zone size increases.

A form of arc welding that has gained popularity recently is manual metal arc welding (MMAW), commonly referred to as shielded metal arc welding (SMAW). First, there was not much advancement in electrical welding after Humphry Davy discovered the short-pulsed electric arc in 1800 and Vasily Petrov discovered the continuous electric arc in 1802, until Auguste de Méritens created a carbon arc torch that was patented in 1881. ensite in the microstructure of steels. A form of arc welding that has gained popularity recently is manual metal arc welding (MMAW), commonly referred to as shielded metal arc welding (SMAW). First, there was not much advancement in electrical welding after Humphry Davy discovered the short-pulsed electric arc in 1800 and Vasily Petrov discovered the continuous electric arc in 1802, until Auguste de Méritens created a carbon arc torch that was patented in 1881. For coating the electrode with carbonates and silicates. Strohmenger introduced a highly covered electrode in 1912, however the early electrodes were not widely used due to their high cost and intricate production processes. The invention of the extrusion process in 1927 allowed producers to create more intricate coating combinations intended for particular uses, while also lowering the cost of coating electrodes. Iron powder was added to flux coating by manufacturers in the 1950s, which allowed for faster welding. Gravity welding, a modern term for an automated SMAW variant, was first described by Karl Kristian Masden in 1945. Its employment in Japanese shipyards brought it notice in the 1960s, when it temporarily acquired popularity; but, these days, its uses are restricted. An additional seldom-utilized form of the procedure is called firecracker welding. Carbon arc welding was created in 1885 by Nikolay Benardos and Stanisław Olszewski, who obtained American patents in 1887 that featured a basic electrode holder. Nikolay Slavyanov created the consumable metal electrode in 1888. C. L. Coffin obtained U.S. patent 428,459 later in 1890 for his metal electrode-based arc welding technique. Melted electrode metal was put into the weld as filler by the method, much like in SMAW.

Many materials, both comparable and dissimilar, can be welded using manual metal arc welding (MMAW). Technology that offers high quality and productivity has been developed with a lot of work. It makes advantage of the particular properties of materials such as aluminum, magnesium, and steel, as well as joining methods (Chaudhary et al., 2021a)

Hard materials are fused together using the MMA welding technique. Because MMA welding produces extremely high temperatures, any non-consumable electrode used in this process needs to have a very high melting point.

The use of coated electrode and an as filler material and electricity is known as the Manual Metal Arc welding procedure. The coating substance provides the shielding gas in the MMAW process. If no shielding gases is employed at welding temperature, ambient gases react with the hot weld metal and create contamination. Important input parameters for the welding process are feed rate, voltage, welding speed, and welding current. These parameters control the mechanical, microstructural, and macro characteristics of the weld. More molten electrode material spreads when the welding voltage is raised because the arc length and weld breadth both increase when the distance between the work piece and the electrode tip increases. If the welding current is high, the heat provided to the weld is likewise high, resulting in greater molten volume, which suggests a rise in one, two, or all three of the weld's essential dimensions. The three most important aspects of the weld are the depth of penetration, weld breadth, and reinforcing height.

Heat input decreases with increased welding speed. The feed rate of the operation has an impact on the volume deposited on the bead per unit of time. The structure of the weld determines its mechanical qualities. The three macroscopic weld properties of the process are the depth of penetration, weld breadth, and reinforcing height. The depth of penetration should be maximized for greater strength, and it should be designed to yield the best depth of penetration given the input parameters. Low carbon steel is the most common form of steel as its price is relatively low while it provides material properties that are acceptable for many applications. In manufacturing operations, many parts and components made of low carbon

steel are formed into various shapes by applying external forces, mechanical properties of materials are the most important parameters taken into account in design and manufacturing of products. Mechanical properties of metals determine the range of usefulness of a material and establish the service life that can be expected. Mechanical properties are also used to help classify and identify the material. The most common properties considered are strength, ductility, hardness, impact resistance, and fracture toughness. Ductility may increase or decrease with increasing temperature depending on the same variables in manufacturing processes especially in metal forming such as bulk deformation processes which include forging, rolling and extrusion, also in sheet metal forming operations, the formability depends on mechanical properties of manufactured metals. Due to high industry importance and wide application of A36 steel, this experimental study was carried out to get the effect of passing the electrical current through steel products during manufacturing, Arc and spot welding, or maintenance. Which can help us to improve the quality and reduce the cost of manufactured products.

1.2 Statement of the Problem

There may be serious financial consequences and human lives put in danger when a structure collapses because of the welded metal losing its mechanical qualities. Consequently, it is imperative to explore methods for enhancing the durability and dependability of welded junctions.

The most frequent reasons for welded structural failure in railroads, ships, construction and mining equipment, agricultural equipment, bridges, and offshore equipment continue to be fatigue failure and welding features, which lead to large costs. These kinds of structures' structural elements and components are continuously subjected to shifting amplitude loading while they are in use. Eighty percent (80%) of the main structures and parts of construction machinery are made of welded steel constructions made from a range of steel grades.

In the case of welding, the parts are joined by means of interatomic metallic contacts, which ultimately create the weld joint. Because component portions have strength equal to or greater

than the constituent components and almost the same, structural composition as the foundation, material, welded connections are favored over bolted joints in many design contexts. One essential component of a steel structure or component is a welded connection. Material properties, such as ductility, ultimate strength, and the relationship between real stress and strain, vary from one place around the weld to another at joints. In actuality, problems with the welding process usually result in the failure of the welded structure. The kind of environment and the materials used determine failure.

Controlling the process input of welding parameters to provide an acceptable welded joint with the necessary strength and little to no negative residual stresses and distortion is currently the most common difficulty that manufacturers are experiencing. To supply sufficient electric current to melt the electrode and the necessary quantity of base metal, the method requires proper control welding settings. Most of the research in the field of welding has concentrated on the characteristics of welding optimization, such as the use of genetic algorithms to optimize gas metal arc welding, the use of grey relational analysis (GRA) and Taguchi method to optimize weld bead geometry during TIG welding, and the use of finite element analysis to analyze residual stress during butt welding two similar plates.

Oxy acetylene (OAW) welding is a straightforward, portable, and inexpensive procedure that has some advantages, but it also results in a large Heat Affected Zone (HAZ) that causes noticeable deformation due to the increased total heat input per unit length of weld. Shielded Metal Arc Welding is another popular welding process (SMAW). It is a process for melting and connecting metals by producing an arc between a stick-like insulated electrode and the metals. Also, the welding equipment is inexpensive, lightweight, and simple to However, the low power density of the heat source is one of the limitations of the two welding techniques covered above. The power density grows from a gas flame to an electric arc, a high-energy plasma, and a high-energy beam. The amount of heat input needed for welding reduces as the heat source's power density rises. The material of the work piece exposed to a gas flame heats

up so slowly that a significant quantity of heat is already carried away into the majority of the work piece before any melting takes place.

Overheating has the potential to weaken and distort the work item. On the other hand, regulating welding parameters such as welding current, voltage, and speed can restrict the amount of heat injected into the weld. Moreover, the quality of the weld can be significantly impacted by edge preparation done before welding.

This research would be very helpful in gaining a better understanding of the mechanical properties of mild steel that influence the service performance of welded joints under the various welding parameters such as welding speed, voltage, arc length, electrode diameter, current, and thickness of the base metal. This is because arc welding processes, like MMAW, provide a broad range of thermal energy for joining different thicknesses of steel.

1.3 Purpose of the Study

The primary goal of this research is to examine how welding parameters affect the mechanical characteristics of low carbon steel when it is welded by hand using a metal arc welding process. The study will be directed by the following precise objectives.

1. To look into the microstructure of the welded LAP and Butt of A36 LCS's HAZ area.
2. To contrast the parent metals and LAP's HAZ's hardness characteristics with those of the butt-welded A36 LCS.
3. To contrast the HAZ of the Butt and LAP joints' tensile characteristics.

1.4 Significance of the Study

First off, the major conclusions of the study might help aspiring welders, producers, and engineers in the welding industry comprehend the importance of welding parameters in preserving the mechanical properties of welded metals and limiting breakdowns and failures of welded structures. Second, other academics working on related topics will use the study's

findings as a guide. Additionally, the study's conclusions and suggestions will broaden the understanding that welding industry stakeholders need to offer affordable, safe goods. Lastly, the study's findings will advance academic literature and understanding among researchers, engineers, and students pursuing degrees in manufacturing, material science, welding and fabrication, and other related fields.

1.5 Scope of the Study

The investigations concentrate on the main variables—welding current, arc voltage, welding speed, polarity, edge preparation, and welding technique—that affect the mechanical properties of welded joints. The main variables that regulate the fusion, penetration depth, weld puddle shape, reinforcing, and heat input are welding current, welding voltage, and welding speed. Secondary variables influencing energy absorption, base metal and weld metal melting rates are electrode polarity, inclination angle, and welding technique.

1.6 Organization of the Study

This work was divided into five chapters. The introduction of the first chapter detailed the study's background, problem statement, goal, specific objectives, significance, and organization. Chapter 2 provides a comprehensive overview of the research objectives and a comprehensive literature review.

Chapter 3 covers the study's supplies and methods. Chapter 4 presents the results and debate, while Chapter 5 concludes with a review of the findings and suggestions for more research.

CHAPTER TWO

LITERATURE REVIEW

2.1 Introduction

One common method for permanently joining various materials is welding. Melting and solidification of the work piece and filler materials occur at the interface during the welding process. A variety of filler materials are added during some welding processes, while other processes weld without the use of filler materials.

Making a joint as sturdy as possible so that it can withstand loads is its primary goal during formation. The least expensive of all the other significant joining techniques is welding. Since the weldability of a certain material determines whether the process is feasible, welding cannot be used to unite all materials. One method of welding could work well.

Welding current, welding speed, voltage, and feed rate are critical inputs for the welding process parameters. These variables regulate the weld's mechanical and microstructural characteristics. As the distance between the work piece and the electrode tip grows, the welding voltage will typically increase along with the arc length and weld width, causing the molten electrode material to spread more widely. When the heat delivered to the weld is high due to high welding current, the molten volume increases, indicating an increase in one, two, or all three of the critical dimensions of the weld. The depth of penetration, weld breadth, and height of the reinforcement are the three crucial weld dimensions.

When welding speed is raised, the amount of heat input

The structure of the weld affects its mechanical characteristics. The depth of penetration, weld breadth, and height of reinforcement are the macroscopic weld characteristics of the process. The depth of penetration should be greatest for larger strength and it should be constructed to attain the best value of the depth of penetration for given input parameters.

Arc effectiveness

The electrode coating provides increased arc thermal conductivity. As a result, electrode coating efficiently prevents the transfer of molten metal from the electrode tip to the base metal, assisting in the increase of welding speed and arc efficiency.

2.1.1 Effect of welding current on the microstructure of different material

The impact of welding current on the microstructure of the material was investigated by the material utilized was Ni-base super alloy with current 55, 80, and 95 A. It was found that when the current was low, not much heat was being injected to boost the temperature. This prevented the formation of a broader and deeper weld pool. It also clarifies the relationship between the welding current and the weld pool's breadth and depth. Both the width and the depth expand with increasing current. When the current is raised even more, stress concentration occurs. In the weld where current increased, dendrite size growth was seen. After doing several tests, he The following factors must be considered:

(a) Rate of temperature rise

(b) Maximum heat input value

(c) Time spent maintaining this temperature peak and

(d) Rate of cooling. The HAZ will be wider the more the supply current is valued.

2.1.2 How welding speed affects various materials' microstructure.

During the process of welding, the material consecutively melts and solidifies with a peak of high power. Several parameters such as the laser energy, pulse frequency, pulse duration, welding power and welding speed govern the mode of the welding process. Due to the decrease in the heat input, welding speed affected penetration depth more than bead width, and a narrow width of heat-affected zone.

Using the various welding speed ranges of 90~180 mm/min with an invariable rotation speed of 950 r/min. The effect of welding speed on microstructure evolution and mechanical properties of the joints was investigated. The results show that, with the welding speed

decreasing, the size of the nugget zone (NZ) first increases and then decreases due to different welding temperatures. At a welding speed of 150 mm/min, the size of the nugget zone(NZ) in all joints is the biggest and the and equiaxed grains are finer, attributed to a higher degree of dynamic recrystallization, and a larger number of fine precipitated phase particles are depressively distributed in the nugget zone. Correspondingly, the joints have the highest tensile properties, and the tensile strength, yield strength and elongation are, respectively, 406 MPa, 289 MPa and 7.2%. However, compared to the base material, the tensile properties of all joints are reduced because a greater amount of particles is dissolved in the nugget zone.

2.1.3 How arc voltage affects certain materials' microstructures

Voltage is one of the most important variables in a welding procedure.

Voltage has a direct impact on heat input. As voltage goes up so does heat input.Heat input can be extremely important when welding materials whose physical and mechanical properties may be affected by it. In some cases, high heat input to slow down the cooling rate and prevent embrittlement. In other case, low heat input to speed up the cooling rate and prevent sensitization cracking. Welding voltage controls the arc length: the distance between the weld pool and the wire filler metal at the point of melting within the arc. As the voltage increases, the weld bead will flatten out, and its width-to-depth ratio will increase. The effects of voltage on the weld's surface, helping it lay flat and wash in at the edges. Too much voltage can produce a weld that is flat, concave or undercut. Too little voltage could yield a shoddy weld bead, or it can contribute to a lack of fusion.

2.1.4 How heat input affects certain materials' microstructures

When heat is applied, austenite concentrations in the weld metals increased and austenite concentration and the fraction -austenite twin-grain boundaries followed the same trends. With increasing heat input, the recrystallized ferrite and austenite grains initially decreased and subsequently increased, whereas the fraction of interphase boundaries between special

ferrite and austenite exhibited the reverse trend. With a heat input of the toughness and plasticity of the weld metals were enhanced by an increase in austenite content, recrystallized grains, and austenite twin-grain boundaries. The plasticity and tensile strength values of the welded metal changed more when the heat input is raised.

The impact of heat input on the mechanical characteristics and microstructure of super alloy. It was discovered that generating a deeper pool and adding enough heat to the weld required an increase in current and a drop in welding speed. Min et al. 2009 studied the change in the microstructure of AZ61 magnesium alloy on the application of heat input. The mean grain size of the base material was 39 lm. Essentially, the a-Mg phase and bMg17Al12 phase were found in the fusion zone (FZ). The size of grains significantly increased in the heat-affected zone (HAZ). The reason behind these grain growths is the high temperature 527 K, which is higher than the recrystallization temperature of magnesium alloys.

2.1.5 How welding current affects various materials' mechanical characteristics

Coarse grain in the microstructure indicates lower hardness and low strength. As increasing of the arc welding current from 70-120A in A36 carbon steel will increase the welding heat input, it will affect the microstructure of the weld itself and give impact on the strength and hardness of the material. The welding current is the variable that mainly controls the amount of weld metal deposited during the welding process. Amperage measures the strength of the electrical current, with its primary effect on welding being the melt-off rate of the electrode and the depth of penetration into the base material. The Microstructure of weldment (WM) and parent metal is known that it undergoes considerable changes because of the heating and cooling cycle of the welding process. A36 carbon steel will increase the welding heat input, it will affect the microstructure of the weld itself and give impact on the strength and hardness of the material. The increase in welding current results in increases in temperature of the weld and results in the depletion of toughness and hardness because of increased cooling time that gives rise to rapid growth of the grain. Thus, the objective of this project that is to investigate the Mechanical

properties of the welded joint part using SMAW and to investigate the effect of current towards the weld is achieved.

2.1.6 How arc voltage affects the mechanical characteristics of certain materials

The micro hardness profiles over the AZ31 pair are displayed in According to these profiles, the base metal zone (75HV) and the heat-affected zone (HAZ) had the highest hardness values, while the fusion zone (50HV) and the heat-affected zone (43HV) had slightly lower micro hardness values. The welding of the FZ and HAZ, which altered their microstructure, caused this variance in hardness. The hardness of an alloy increases with the amount of hard particles present and decreases with the size of the grain and effects of electrical energy on the most important properties of low carbon steel such as yield strength, ultimate strength, hardness, and impact strength. These properties are the most important parameters of design and manufacturing of machine parts and structures. A36 is one of the low carbon steels that are widely used in different industries. The chemical composition of this steel includes carbon between0.17 and 0.2 (% wt.). Present work focuses on the relationship between the change of mechanical properties of steel and electrical power passing through its products. Experiments show that increasing current or voltage passing through products made of this type of steel results in decreasing of their mechanical properties.

2.1.7 Feed rate's impact on penetration depth

Higher feed rates increase weld metal deposition and increase current since melting rates at the end of the wire must increase as the wire feed increase. As a result, the semi-automatic processes, current is typically adjusted by changing the wire feed speed since the two are relatively proportional. The electrode is melted by the arc heat and transferred to the molten pool in the form of droplets. On every occasion that a droplet breaks away from the electrode tip the arc length varies intermittently. Accordingly, the size and the shape of the transferring droplets and the transfer frequently dominate the welding arc stability and thus affect the worker ability and weld quality. The wire or electrode size of droplets transferred from

electrode wire tip becomes either too large or irregular, the arc length associated with the droplet transfer and fluctuation of arc position becomes large and the arc becomes unstable

The melting rate of the electrode is directly related to the quantity of deposited metal per unit time and controls the welding efficiency. The melting rate of the electrode or rod is directly related to the quantity of deposited metal per unit time and controls the welding. The electrode droplets transfer phenomena vary according to numerous operational factors such as current, voltage, polarity, shield gas, materials and type of wire extension (solid or cored), wire diameter and base metal.

2.1.8 The impact of welding speed on penetration depth

The overall trend for all the experiments in our investigation showed that the depth of penetration reduced as welding speed increased if the input current, input voltage, and feed rate were fixed at 100 A, 9.0 V, and 2.12 mm/s, respectively. The depth of penetration decreased from 1.76 mm to 1.74 mm if the welding speed was increased from 1.19 mm/s to 1.44 mm/s; the depth of penetration decreased from 1.74 mm to 1.71 mm if the welding speed was increased from 1.44 mm/s to 1.82 mm/s; and the depth of penetration again decreased from 1.71 mm to 1.65 mm if the welding speed again decreased from 1.82 mm/s to 1.91 mm/s. In actuality, the volume of the weldment reduces as welding speed increases because the heat rate drops and produces less molten volume. This shows that when welding speed increases, the weld width, penetration depth, and reinforcement height decrease. Since the weld volume is proportionate to all three of these weld parameters, this change is consistent with convention.

2.1.9. The impact of welding voltage on penetration depth

The depth of penetration reduced as the voltage increased for our study range if the welding current, welding speed, and feed rate were all fixed at 100 A, 1.19 mm/s, and 6.35 mm/s, respectively, and only the welding voltage was raised. The depth of penetration dropped from 1.44 mm to 1.37 mm when the voltage was increased from 9.6 V to 10 V, from 1.37 mm to 1.31 mm when the voltage was increased from 10 V to 10.5 V, and from 1.31 mm to 1.25 mm

when the welding power was again increased from 10 V to 10.5 V. This makes sense since when the voltage rises, the input heat rises as well.

2.1.10. Welding current's impact on penetration depth

The depth of penetration varied each time if the welding voltage, speed, and feed rate were maintained at 9.6 V, 1.44 mm/s, and 6.35 mm/s, respectively, and only the welding current was altered. Increases in current from 100 A to 125 A resulted in an increase in penetration depth of 2.73 mm to 2.81 mm; similarly, an increase in current from 125 A to 150 A increased penetration depth from 2.81 mm to 2.87 mm; and still another increase in penetration depth from 2.87 mm to 2.89 mm occurred when current was increased from 150 A to 200 A. This suggests that, under the parameters of our investigation, penetration depth rises as current level One explanation for this is that when the current is raised, the input heat and melted volume also rise. Consequently, one, two, or all three-bead dimensions will grow since the volume of the bead is directly proportional to the product of the three bead dimensions. This suggests that the depth of penetration fluctuation with current follows convention.

2.2 Welding joint types (Process Parameters for MMAW)

As illustrated in figure 2.13, the American Welding Society lists the five main types of welding joints as butt, corner, lap, tee, and edge joints.

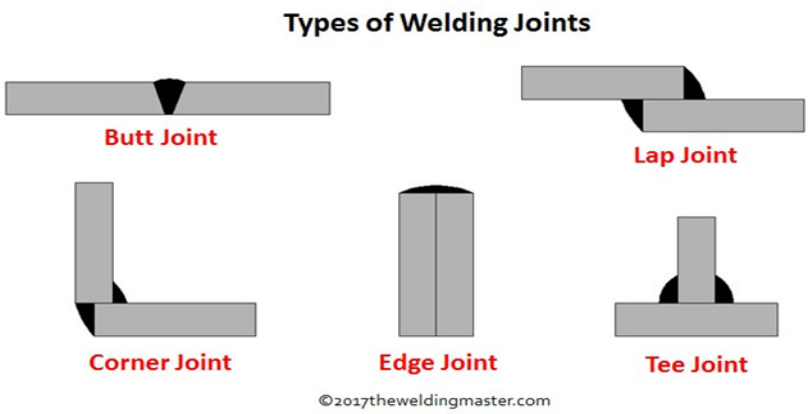

2.2.1 Butt joint

The joint that is formed by placing the ends of two parts together is called butt joint. In butt joint, the two parts are lie on the same plane or side by side. It is the simplest type of joint used to join metal or plastic parts together. The different weld types in butt-welding are Square Butt weld, Bevel groove weld, V-groove weld, J groove weld, U-groove weld, Flare-V-groove weld and Flare-bevel-groove butt weld.

2.2.2 Corner Joint

Corner joints are created when two parts are placed at a right angle to one another. The shape of an L is formed by two pieces that will be welded together at the corner. The following are the many types of welds used in corner joints: The following types of welds are available: Fillet, Spot, Square Groove, Bevel-groove, U-groove, J-groove, Flare-V-groove, Edge, and Corner-flange.

The joint formed by two components meeting at a right angle, or 90 degrees, with one portion located in the middle of the other. The two parts that are welded together to resemble the English letter "T" are termed T joints. T-joint welds come in the following varieties: melt-through, J-groove, fillet, plug, bevel-groove, and flare-bevel groove.

2.2.4 Lap Joint

After the two pieces are stacked one on top of the other and fused together, the lap joint is created. It could have two sides or only one. The most common application for these kinds of welding joints is the joining of two pieces of varying thickness. There are several types of welds used in lap joints, including fillet, flare-bevel-groove, plug, slot, J-groove, and spot welding.

2.2.5 Edge Joint

An edge junction is created by joining two pieces together by welding their edges. When two sheets' edges are roughly parallel planes at the welding point and they are adjacent, this junction is employed. This joint cannot be utilized to apply tension or pressure because the

weld does not fully penetrate the thickness of the joint. The several types of welds used in this welding connection include butt welds, edge flange welds, corner flange welds, V-groove welds, J-groove welds, and U-groove welds

2.2.6 Justification for choosing low-carbon steel

Since low carbon steel produces a homogenous and stronger casing and is very wieldable, it is said to be the best steel for carburized parts. Low carbon steel offers a good balance of strength, ductility, and toughness. Low carbon steel has superior mechanical properties in addition to superior machining capabilities and Brignell hardness. This steel alloy has a small amount of manganese added to it to aid in achieving these properties. Low carbon steel is less expensive because it is simpler to produce and grind. Because of its qualities, low carbon steel is ideal for many different types of parts, such as spindles, sprockets, rods, shafts, and pins. The primary ingredient in this material is iron. By weight, the carbon concentration ranges from 0.14 to the addition of between 0.6 to 0.9 percent by weight of manganese helps to increase hardness. Low carbon steel's chemical makeup produces a robust and ductile material with comparatively low toughness and hardness when compared to other alloys.

Table 2.1 Mechanical Properties of Low carbon steel

Sl. No.	Mechanical Properties	Range
1	Shear Modulus	80 GPa
2	Machinability	70%
3	Poisson Ratio	0.290
4	Bulk Modulus	140 GPa
5	Modulus of Elasticity	205 GPa
6	Yield Strength,	370 MPa
7	Elongation	15.0%

8	Ultimate Tensile Strength,	440 MPa
9	Vickers Hardness	131
10	Rockwell Hardness	71
11	Knoop Hardness	145
12	Brinell Hardness	126

2.3 Welding Current

As demonstrated in among the several welding factors, such as welding current, voltage, and speed, welding current is most likely the one that influences weld penetration, deposition rate, weld bead geometry, and weld metal quality. On the other hand, the weld bead width is directly impacted by arc voltage. The width of the weld often increases with an increase in arc voltage. The main function of welding current is to control the penetration and overall size of the weld bead. Insufficient welding current causes the weld metal to pile up as a bead on the faying surface rather than piercing the work piece. Under these circumstances, the weld bead's reinforcement is increased without sufficient penetration. Weld sag is the result of the work piece being overheated by an excessively high welding current.

Effect of welding current on melting of electrode of different diameters.

The most significant influence on the deposition rate, the size, form, and penetration of the weld bead is the welding current employed in MIG. In MIG welding, metals are often welded with direct current polarity electrode positive (DCEP, in contrast to TIG welding), as this allows a reasonably deep penetration to be achieved and maximizes heat input to the job. The DCEP's oxide elimination function helps to clean the weld deposit and is particularly significant when welding magnesium and aluminium alloys. Increasing the current will result in larger weld beads and deeper and wider weld penetration when all other welding parameters remain unchanged. When operating at a constant voltage, the wire feed speed.

2.3.1 Welding Voltage

One of the most crucial MMAW variables that needs to be kept under control is the arc length. The arc length and arc voltage are directly associated when all other variables, including the types and composition of electrodes, the welding technique, and electrode coating, are held constant. An arc with a considerable length disrupts the gas shield because it tends to stray and interferes with the penetration and bead surface. The arc voltage in MMAWs has a significant impact on the penetration, bead width, and bead reinforcement. The weld bead gets flatter and larger as the arc voltage increases, and penetration rises until the voltage reaches its optimal value, at which point it starts to fall.

2.3.2 Travel Speed

The rate at which the arc moves along the work piece is known as the travel speed. In semiautomatic welding, the welder controls it, whereas in automatic welding, the machine does. The effects of the arc voltage and the travel speed are quite comparable. As the arc speed is changed, the penetration reaches a maximum at a given value and then diminishes. Because slower transit speeds result in longer heating times, they correspondingly produce larger beads and more heat input to the base metal for a given constant current. A broader bead shape is the result of the high heat input's increased weld penetration and weld metal deposit per unit length. A strange weld build-up happens if the travel speed is too slow.

2.3.3 Electrode Size

The weld bead configuration, including size, depth of penetration, reinforcement, and width, is influenced by the electrode diameter, which in turn affects the welding travel speed. As the electrode diameter gets smaller, the arc gets more piercing for the same welding current. In general, a larger electrode needs a greater minimum current to have the same properties. The smallest wire that allows for the required weld penetration should be used in order to get the highest deposition rate at a given current. Broader electrode diameters produce welds that are wider in breadth but have less penetration. The desired weld penetration, the thickness of the

work-piece to be welded, and the wire electrode diameter all influence the choice of electrode size.

The mechanical and structural characteristics of heat affected zone

The heat affected zone (HAZ) and the metallurgical characteristics of the weld metal are crucial because they directly affect the mechanical characteristics and joint performance of the weld. It is well known that the distributions of pearlite, ferrite, and grain size in base metal and HAZ vary depending on the type of weld condition utilized. In a single welding touch pass, the material is quickly heated to its maximum temperature, after which it is permitted to cool more slowly because of heat conduction into the parent metal's bulk. Temperature-related phase changes are possible. If the material is far enough away from the weld pool, it is unharmed. Heat and sacks produced during the welding process will have an impact on the metal properties. Weld microstructure, which is affected by flux, base metal composition, wire electrode composition, and cooling conditions, has a significant impact on these mechanical properties. Furthermore, the mechanical properties and microstructure of the weld are affected by welding process variables, both directly and indirectly. The impacts of two fluxes with varying basicity were investigated using two experimental wires and a Columbian bearing base plate. The results showed that the flux basicity affected the microstructure, impact properties, and the transfer of the hardenability element of the weld deposit. Instead of focusing on metallic inclusions, quantitative image analysis was used to examine the impact of flux basicity on microstructure. It was shown that the filler material and flux composition in SMAW affected the creation of the notch's toughness is demonstrated.

2.3.4 The Value of the Zone Affected by Heat

Heat Affected zone with a sensitive toughened microstructure that benefits from higher cooling rates and carbon equivalent values (CEV) of 14. Up until recently, the only quality about the HAZ was its ability to withstand spasmodic hydrogen cracking. The relative defect tolerance of the

nd welding. The procedure that was employed was called shielded metal arc welding (SMAW), which entails creating an arc between a work piece and a covered metal electrode. Due to their accessibility and broad range of applications in Ghana's and other countries' medium- and small-scale metal fabrication industries, these materials and welding techniques were chosen. It is critical to initially determine the experiment's welding circumstances before delving into the characteristics of the heat-affected zone. As a result, it was determined that three welding parameters—arc voltage, welding speed, and welding current—had the greatest impact on the overall quality of the weld. Next, utilizing shielded metal arc welding technology, the optimization of welding parameters for weld bead quality was examined. This modifies the system to guarantee that the experiment sample's welding process travels at the ideal welding current and speed. Straight welds are frequently produced using SMAW with the same welding machine and electrode that are used to create final experiment samples. The work pieces are then clamped in a steady position on the working bench. The test samples used for this work's optimization of the welding parameter were made using A36 LCS and an electrode identical to AWS E6013.

3.2 Resources

For the experiment, an A36 LCS plate with a thickness of 5 mm × 40 mm × 100 mm was utilized. This is taken into consideration due to its widespread application in the manufacturing sector. It provides an excellent mix of ductility, strength, and toughness. For the three investigations, eighteen (18) samples were prepared: six (6) samples for each of the three tests (tensile, hardness, and microscopic). Using tensile and hardness testing apparatus, the mechanical properties both before and after welding were examined.

The tensile test was conducted using the AVIC International WAW-1000B universal tensile testing apparatus. The depth of indentation around the HAZ in relation to the other locations

was also measured using hardness testing equipment. The A36 LCS plates were joined using the SMAW method.

3.2.1 Material: A36 Low Carbon Steel

One of the most popular steel grades is A36 LCS. It provides an excellent mix of ductility, strength, and toughness. It gives a consistent and tougher finishing and is very weldable. A36 LCS's Mechanical Properties

A36 steel's ultimate tensile strengths might vary from 58,000 to 79,800 psi. The exact ultimate tensile strength is dependent upon several factors, such as the composition of chemicals and the method of formation. A36 is relatively ductile and can stretch to around 20% of its original length when put through tensile testing. Because of its strength and ductility, it possesses good impact strength at room temperature.

A36 LCS's Mechanical Properties

A36 steel's ultimate tensile strengths might vary from 58,000 to 79,800 psi. The exact ultimate tensile strength is dependent upon several factors, such as the composition of chemicals and the method of formation. A36 is relatively ductile and can stretch to around 20% of its original length when put through tensile testing. Because of its strength and ductility, it possesses good impact strength at room temperature.

Table 3.2 Mechanical Properties of A36 LCS

Mechanical Properties	Metric	Imperial
Ultimate Tensile Strength	400 – 550 MPa	58,000 – 79,800 psi
Yield Tensile Strength	250 MPa	36,300 psi
Elongation at Break (in 200 mm)	20.0%	20.0%
Elongation at Break (in 50 mm)	23.0%	23.0%
Modulus of Elasticity	200 GPa	29,000 ksi
Bulk Modulus (Typical for steel)	140 GPa	20,300 ksi
Poisson's Ratio	0.260	0.260
Shear Modulus	79.3 GPa	11,500 ksi

A36 steel is used for many different purposes in many different industries due to its low cost. As previously mentioned, its mechanical properties make it particularly well-suited for structural uses. A36 steel is a common material used in bridge building. Because A36 steel is so strong and durable, it is frequently used to build buildings. A36 steel is also used to make parts for the building, heavy equipment, automotive, and oil and gas industries.

3.2.1 A36 LCS's Chemical Composition

A36 is a low carbon steel. Low carbon steels are defined as having less than 0.3 percent carbon by weight. Because of its excellent welding properties and suitability for drilling, machining, punching, grinding, and tapping operations, it is an excellent all-purpose steel. Furthermore, heat treatment has minimal to no effect on A36 steel because of its low carbon concentration. A36 steel frequently contains trace levels of manganese, sulfur, phosphorus, silicon, and other alloying elements like nickel, vanadium, chromium, and molybdenum. Alloying elements are added to A36 steel to give it the required chemical and mechanical qualities. Because there are no appreciable amounts of nickel or copper in A36, it has poor corrosion resistance.

Table 3.3: Chemical Composition

Element	Chemical Symbol	Content (%)
Carbon,	C	0.25 - 0.290
Iron	Fe	98.0
Manganese,	Mn	1.03
Phosphorous,	P	0.040
Silicon,	Si	0.280
Sulfur	S	0.050

Table 3.4 Physical Properties of A36 LCS

Physical Properties	Metric
Density	7.85 g/cm^3
Colour	Gray

3.3 Uses for Low Carbon Steel A36

Low carbon steel is used in a wide range of industries. LCS is typically utilized in swaging, crimping, and bending operations. Worms, gears, pins, dowels, non-critical pieces of tool and die sets, tool holders, pinions, machine parts, ratchets, and chain pins are among the items that use carburized parts. For fittings, mounting plates, and spacers, LCS is frequently utilized. It works well in applications where high carbon and alloy steel strength are not requirements. Components such as worms, dogs, pins, liners, machinery parts, special bolts, ratchets, chain pins, oil tool slips, tie rods, anchor pins, studs, etc. can benefit from LCS's high surface hardness and soft core. Enhancing drilling, machining, threading.

Figure 3.10 shows the SMAW's electrode, E 6013

3.4 Electrode for Welding

With its excellent welding technological features, consistent arc, minimal splash, and attractive design, carbon steel welding electrodes are ideal for use in a variety of job locations. These characteristics led to the selection of mild steel welding electrodes AWS E6013 by Shijiazhuang Shiqiao Electric welding material CO, LTD., China.

Table 3.5: Electrode conditions (Fekadu, 2018)

Electrode type	**E 6013**
Electrode diameter	3.2 mm
Electrode extension	20 mm
Electrode feed rate	180 mm/min
Work angle	30^{o} from vertical
Type of welding	Flat

3.5 Safety Measures Employed Throughout the SMAW Procedure

The safety of the welder was the most crucial factor. Not only does arc welding use a lot of electricity, but it also emits lethal sparks. The splashes and sparkles could cause damage to

human eyes. Consequently, personal protective equipment such as welding boots, overcoats, welding masks, helmets, gloves, and safety glasses were employed.

3.6 The experimental process

The A36 LCS plate was measured and cut to the required sample sizes of 100mm x 50mm x 5mm at the Welding and Fabrication Department Workshop of Kumasi Technical Institute using an ACCURSHEAR 82506 power-cutting machine. To keep contaminants out of the molten metal

SMAW is notorious for releasing many sparks, which might quickly burn any exposed skin on a person. Therefore, in order to avoid any danger, the complete body needed to be shielded. Splashes during the welding process also carry the risk of starting a fire. All flammable materials were kept a safe distance apart to avoid similar incidents.

Before welding, the specimens were cleared of dust and oil to prevent contaminants in the pool of molten metal. The plate was fastened in place using tack welding to provide the necessary joint arrangement. The work parts are then secured in place on the working bench to prevent joint deformation. The work pieces were maintained in their relative positions while the welding was being done.

The Kumasi Technical Institute's Welding and Fabrication Department workshop was the site of the welding procedure. Shielded metal arc welding was used to join the specimens (SMAW). The test specimens were fused together using **Miller welding machine** and Butt and LAP welding joint designs.

Rectifiers for SMAW coated electrode welding are found in Canon power sources.

Figure 3.11: Accurshear Power Cutting Machine for cutting plate

Figure 3.12: Miller Electric Welding Machine used for the arc welding process.

Table 3.6: Specification of welding machine (Miller -524D)

Input power	**22.8 KVA – 13 KW**
Maximum input current	**57 A – 30 A**
Input voltage	**bi tension 230 V three phase 400 V**
Effective input current	**34 A – 19.5 A**
Welding current range	**50 A – 325 A**
Connector size	**13 Mm**

3.6.1 Joining the Sample

Keeping all necessary safety precautions in mind, the quantity of samples required for the experiment was determined. To weld each joint, the electrode was moved steadily, 90 amps of welding power was applied, and one pass was made.

In order to observe its influence when this parameter is at optimum or below and above the optimum values by adjusting the current values, the welding voltage was held constant at the tested welding current value set combining optimum currents determined by varied thickness. The linear pace at which an arc is pushed along the weld joint is known as the welding speed. With any combination of welding voltage and welding current, the effect of adjusting the welding speed confirms to a general pattern. Welding speed influences weld penetration more than any other variable except current. The optimized welding speed was determined by experimentation, and the voltage was maintained at the ideal level.

Table 3.7: Parameters for LAP Welding

Sample No.	Welding Current (A)	Welding speed(mm/min)	Range
1	90	20	Fast
2	90	25	Moderate
3	90	30	Slow

3.6.2 Calculating Design.

For the most part, fabricators don't usually worry about heat input. However, it is crucial to take the heat input into account when welding metals since the welding process can have a substantial impact on the microstructure. Because it significantly affects the cooling rate, heat input is important in some applications. Faster cooling rates typically produce embrittlement in the heat-affected zone, which is harmful to a weldment. An illustration of this is when

working with materials that are prone to hydrogen-induced cracking, where it is essential to apply enough heat. The welding speed was determined by utilizing Equations 3.1 and 3.2.

$$\boldsymbol{Travel\ Speed} = \frac{Length\ of\ Weld}{Time\ to\ weld}$$

$$\boldsymbol{Heat\ Input} = \frac{Voltage \times Amperage \times 60}{Travel\ Speed\ (In/min\ or\ mm/min)}$$

3.6.3 Tidying up the work piece.

Slags that developed on the weld bead were removed using a wire brush and chipping hammer after the welding operation. Furthermore, a chisel and wire brush were used to clean the work piece that had splashes and sputters from the welding operation.

To prevent variations in internal characteristics that could arise from the cooling rate following the welding processes, each sample specimen was allowed to cool under the same ambient circumstances (still air) after all welding procedures were finished. The shielded metal arc

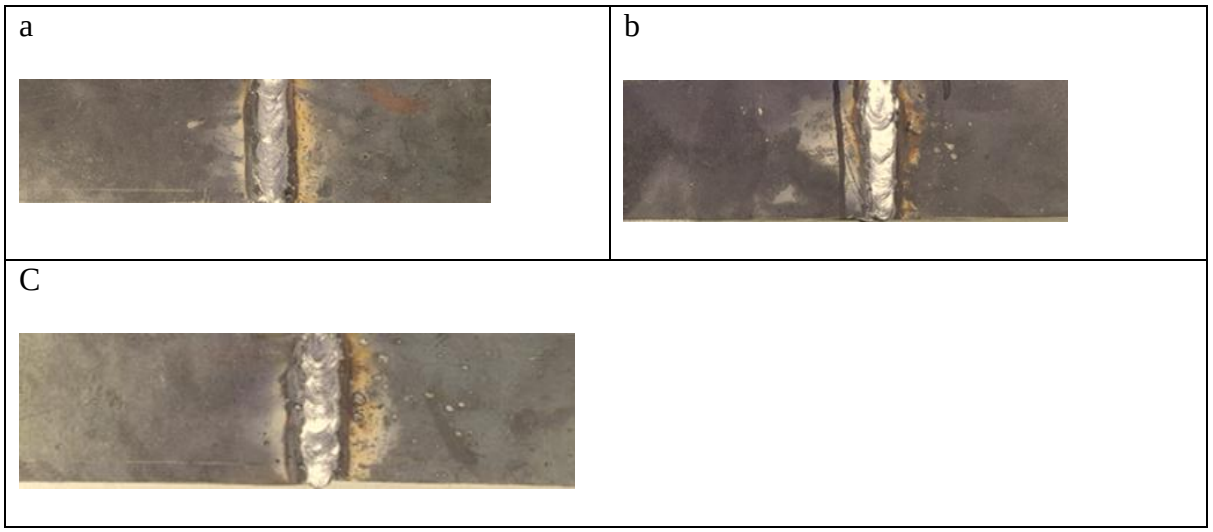

welding method's welding parameters are shown in the table below.

Figure 3.14: A36 Low Carbon Steel Butt weld joint(5mm) a) slow b) medium c) fast

3.7. Tensile test experimental setup description

Tensile and bend tests are most commonly performed using the universal testing machine configuration. For tensile testing, the apparatus comprises replaceable jaws that can grasp both flat and cylindrical specimens. The machine's lower part contains attachments for performing bend tests. The experimental data are displayed on the updated testing machine's monitor after the results are copied from the processing unit.

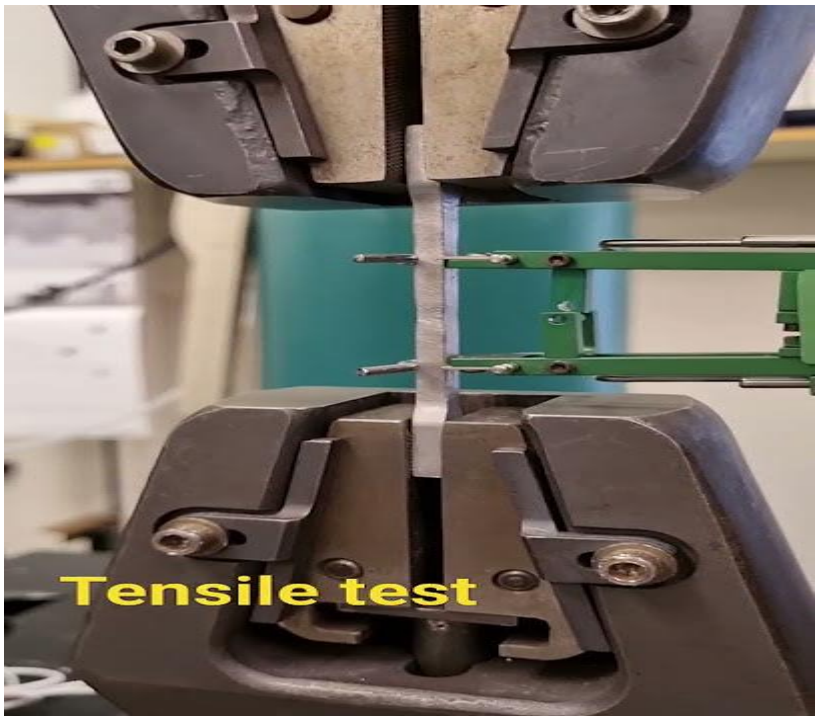

Figure. 3.*15*: Universal testing machine – model WAW-1000A

Figure 3.16: HAZ Sample test specimens for tensile testing

Three (3) sample specimens totalling six (6) pieces of butt and LAP joints fabricated utilizing the shielded metal arc welding procedure were used in the experiment. Prior to conducting the tensile and bend tests on the sample specimen, a digital balance was used to measure each specimen's weight. The weight recorded for each sample was then utilized to determine its density. A representative specimen is weighed in Fig. 3.9. A universal tensile testing machine, the WAW-1000A Sunyani Technical University, was used to conduct the tensile tests. A sample of the specimen was used to hold the top and lower jaws of the tensile testing apparatus in place while it was tugged to failure. Every one of the six (6) sample specimens had this done for them. As seen in Figure 3.10.

Figure 3.17: Digital balance was used to take mass samples before and after testing

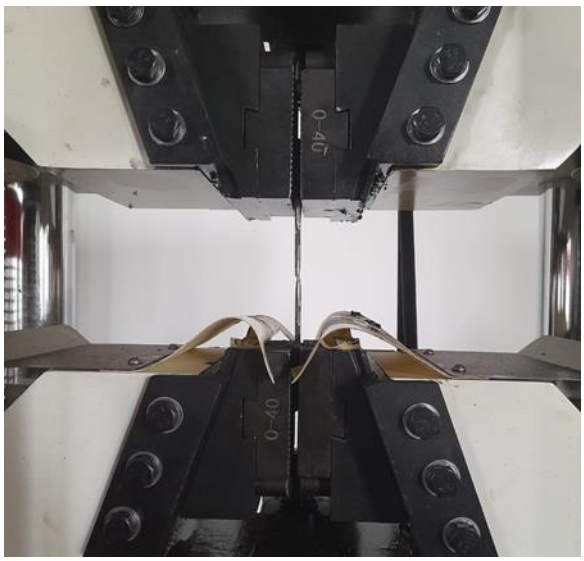

Figure 3.11: Specimen after failure during tensile testing

3.7.2 The Hardness Test's Experimental Method

The experiment made use of three (3) sample specimens and six (6) pieces of HAZ-produced butt and LAP joints that were fabricated using the shielded metal arc welding technique. A material's hardness determines how well it withstands abrasion, cutting, scratching, and penetration. It is a material's ability to withstand ongoing deformation. There are numerous hardness tests available, including the Vickers, Brinell, and Digital B Rockwell tests. AVIC

International's Digital B Rockwell Hardness Testing Machine was used to evaluate the specimens' hardness in compliance with the THRP-150D standard.

The sample specimens were positioned so that their surfaces were on the anvil, and they were lifted to the point where they touched the indenter by gradually rotating the hand wheel. The specimen's surface needs to be prepared such that the ends of the indentation diagonals are distinct. The surface must be carefully prepared to prevent tempering during grinding or work hardening during polishing. A surface grinder with enough coolant must also be utilized. There are two main parameters to test based on the hardness test results. Measuring the width of the heat-affected zone and analysing the change in hardness in the weld heat-affected zone every one of the six (6) sample specimens had them completed. Figures 3.12 shows the experimental configuration.

Figure 3.12: Digital B Rockwell Hardness Testing Machine.

3.7.3 Examination of Metallography

TYM-2A-compliant welds were used to create metallographic samples. Pre grinding, polishing and etching were conducted. The surface was etched using 90% ethanol alcohol and 10% nitric acid to prepare it for metallographic examination of the parent metal and butt welds. The AVIC INTL Digital Photography Metallographic Microscope mode TMR1700 at Cape Coast Technical University was used to examine the parent metal and HAZ. Sectioning was the first step in the creation of a metallographic specimen. A power hacksaw was used to remove a convenient size that included the base metal, HAZ region, and weld metal in order to obtain a representative specimen from the bulk-welded specimens. Following sectioning, the samples were polished, ground, and then etched to reveal the microstructure.

The samples' microstructural pictures were examined under a microscope at various locations within the sections of the samples that were of interest for the investigation (i.e., the weldments, HAZ, and the parent metal). The microscope's attached camera was used to take pictures. Since the specimens were large enough to handle easily during the preparation and examination operations, mounting was not necessary. To improve safety and prevent damage to the preparation-related papers and cloths, sharp edges and corners were removed.

Figure 3.13: AVIC INTL Digital Photography Metallographic Microscope

CHARPTER FOUR

RESULTS AND DISCUSSSION

The data gathered from the experiments and a thorough analysis of the experiment's outcomes are presented in this chapter.

At the Cape Coast Technical University AVIC Laboratory, tests for both hardness and tensile strength were conducted. A tensile testing machine with the model WAW-1000B, a maximum force of 1000 KN, a measuring range of 100 – 1000 KN, and a manufacturing number of JN210241X was utilized to evaluate the qualities of the tensile. The test configuration was the Digital B Rockwell Hardness Test. The devices show the test results on a computer monitor while they are being tested.

The experimental work completed in Chapter Three is presented here, along with a discussion of the findings. The presentation of the findings and discussion adheres to the goals of the investigation. This chapter presents the findings of the microstructure analysis of the welded A36 low carbon steel (LCS) LAP and Butt joints surrounding the Heat Affected Zone (HAZ), as well as the mechanical characteristics of the zone, including the hardness and tensile properties of the two joint designs.

4.1 Microstructure Analysis of the Hazard of A36 Low Carbon Steel (LCS)

Microstructure is one of the methods for analysing the characteristics of a material. Owing to phase shifts brought about by the welding process, weld specimens may exhibit significant microstructure differences throughout.

4.2 Base metal

The typical microstructure of low carbon steel (base metal) is ferrite with small patches of pearlite (α-Fe + 〖Fe〗 3 C) around grain boundary edges and corners, as seen in Figure 4.1.

Furthermore, the macro section of a deep penetration LAP weld of carbon steel is shown in Figure 4.1. The borderlines are apparent in this shot (Tadavi et al., 2017).

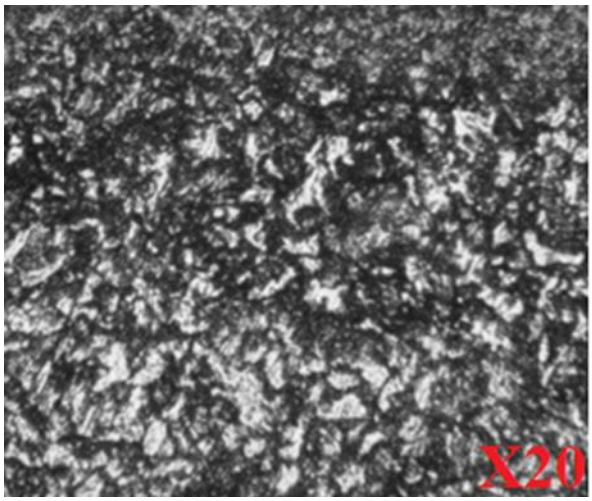

Figure 4.1: Optic4.2.1 The joint HAZ of A36 LCS LAP microstructure

The optical micrograph of the welded A36 LCS LAP joint's HAZ is displayed in Figure 4.2. The direction of heat flow is responsible for the elongated ferrite grains that are seen in the micrograph in the area next to the hot zone. At the fusing line, huge granules were seen pointing in the direction of a significant heat flow. This microstructure agrees with the research conducted by (Tadavi et al., 2017). Al microstructure of low carbon steel (Parent metal)

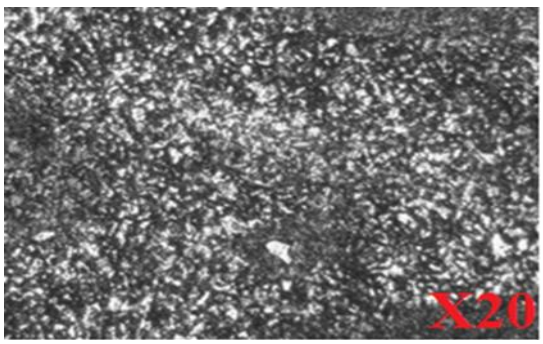

Figure 4.2: Optical Micrograph of HAZ of A36 LCS LAP joint.

The microstructure of the heat-affected zone includes some pearlite colonies in addition to Widmanstatten ferrite, as seen by the micrographs in Figure 4.2. (Tadavi et al., 2017). Adjacent

to the fusion zone is a coarse-grained area of the heat-impacted zone. The grains in this area are somewhat larger than those in base metal.

Once more, Figure 4.2 shows that the centre of the weld is distinct from the other zones. Pseudo-grains and microstructural variability caused by faster cooling rates are the reasons behind this. The results show that this zone is primarily composed of ferrite with a small number of pearlite colonies. The main reasons for microstructural variability during cooling are temperature and chemical gradients.

4.2.2 The optical microstructure of the butt joint HAZ of A36 LCS

According to metallographic research, homogeneous long dendrites produced during traditional butt-welding are a sign that a uniform solidification process took place. That is what **Figure 4.3** depicts. Long dendrites reveal the weld joint's coarse structure. The uniformity of the solidification process is demonstrated by the microstructure.

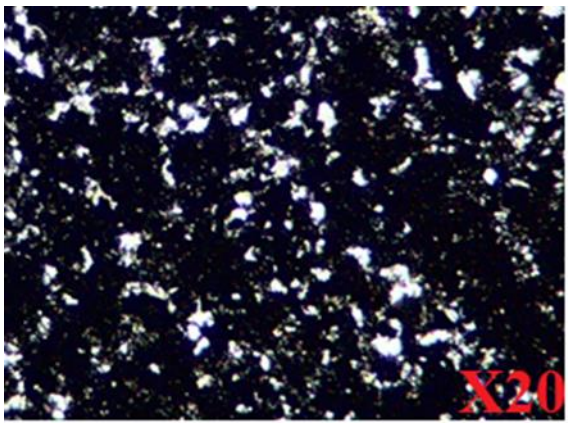

Figure 4.3: Optical Micrograph of welding of A36 Low carbon steel Butt joint.

The microstructure of a mild steel plate that was welded by hand metal arc welding is examined in Figure 4.4, along with the microstructures of each specimen at the weld, heat affected zone, and parent metals. According to the investigation's findings, ferrite and small pearlite (α-Fe +

Fe3 C) patches can be found close to the corners and edges of grain boundaries in BM. Additionally, the LAP demonstrates that the direction of heat flow is what causes the elongated ferrite grains that are apparent in the shot of the area nearest to the HAZ, whilst the butt-welding of the uniform long dendrites indicates that a uniform solidification process took place.

A B C

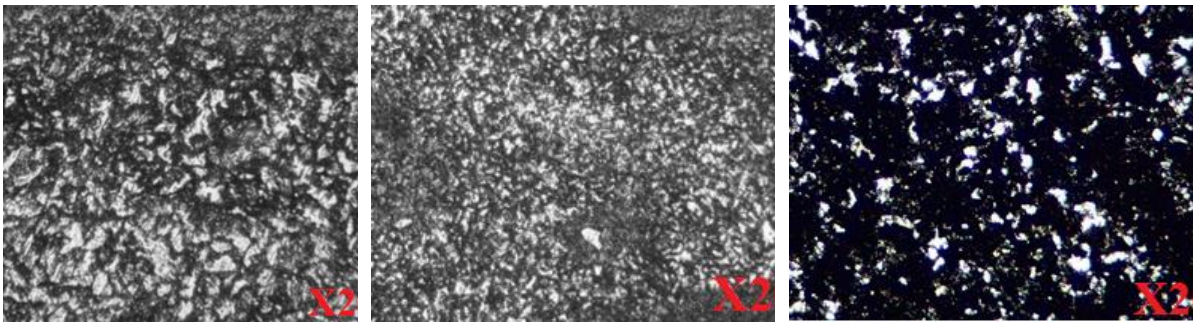

Figure 4.4: Microstructure of (a) parent metal, (b) LAP HAZ and (c) Butt HAZ

4.3 Examining Hardness

4.3.1 Rockwell Hardness Test in the Butt Joint and LAP Hazard Area

Table 4.1 displays the hardness profiles of the three (3) test pieces for the Butt and LAP joints, respectively, across the HAZ. A number of factors, including residual stresses that arose immediately after welding, temperature differences that caused variance in the microstructure of the heat-affected zone (HAZ), and cooling rate—all contribute to the variation in stress across the weld, as Table 4.1 illustrates. The difference in stress across the weld, as opposed to HAZ, which has an average value of 107.7 HRB for the LAP joint and 123.33 HRB for the Butt joint, can be ascribed to a number of things, including residual stresses that form shortly after welding.

Since hardness is also a measure of dislocation density, it is commonly assumed that maximum hardness correlates to compressive residual maximum stress, despite the fact that a variety of parameters, including microstructure and phase composition, can influence hardness. Consequently, the current study's observed hardness profile.

The hardness is practically constant, but there is a noticeable increase on the parent metal near to the weld metal (HAZ) as indicated by the graph connecting the distances from the weld center and HAZ. This is because of the thermal gradient created by the welding heat and the surrounding air temperature, which raises the hardness of the HAZ by producing a martensitic structure (Fekadu, 2018).

For SMAW, a recommended traveling speed is 3 to 6 inches per minute (ipm) / 75.

Table 4.1: Indentation values of Rockwell hardness (HRB) for Butt Joint HAZ

SAMPLE/HARDNESS	HRB	HRB	HRB	HRB	HRB	HRB	HRB	AVERAGE
SAMPLE 1	75.60	55.70	118.50	130.00	126.30	126.90	100.50	104.78
SAMPLE 2	124.90	122.20	125.50	151.40	123.10	129.20	107.10	127.61
SAMPLE 3	114.90	126.60	126.60	122.90	121.00	117.90	127.80	122.53

Table 4.2: Indentation values of Rockwell hardness (HRB) for LAP Joint HAZ

SAMPLE/HARDNESS	HRB	HRB	HRB	HRB	HRB	HRB	HRB	AVERAGE
SAMPLE 1	100.00	99.90	100.00	100.00	100.00	100.00	100.00	99.98
SAMPLE 2	61.30	72.40	86.47	70.00	82.60	70.00	130.00	81.82
SAMPLE 3	94.90	86.20	109.20	91.80	107.60	180.00	129.00	114.11

4.3.2 Hardness Value Analysis for Butt and LAP Joint at HAZ

The hardness values for LAP and Butt joints obtained from the experiment is shown in **Figure 4.6**. The plot was because of changes in hardness of the test specimen.

A graph of hardness was plotted against speed taking into account the two welded joints (Butt and LAP. From the graph, blue and red colours have been used to represent LAP and Butt joint HAZ, respectively. It is clearly shown from the hardness value analysis that, for the sample 1,

the Butt recorded a slightly higher hardness value of 104.78 N/mm^2 as compared to the LAP that was 99.98 N/ mm^2. For the sample 2 joint HAZ for both LAP and Butt, the hardness value for the LAP was 81.82 N/mm^2 and the Butt also recorded hardness value of 127.61 N/mm^2. Lastly, the sample 3 joint HAZ recorded the following values, 114.11 N/mm^2 for LAP and 122.53 N/mm^2 for the Butt weld. Based on the figures obtained, it is evident that apart from all the sample value shown, the Butt recorded a higher hardness value in all the welding joints HAZ than their LAP joint counterpart. Which clearly prove that the Butt welded joint HAZ is harder than the LAP joint HAZ.

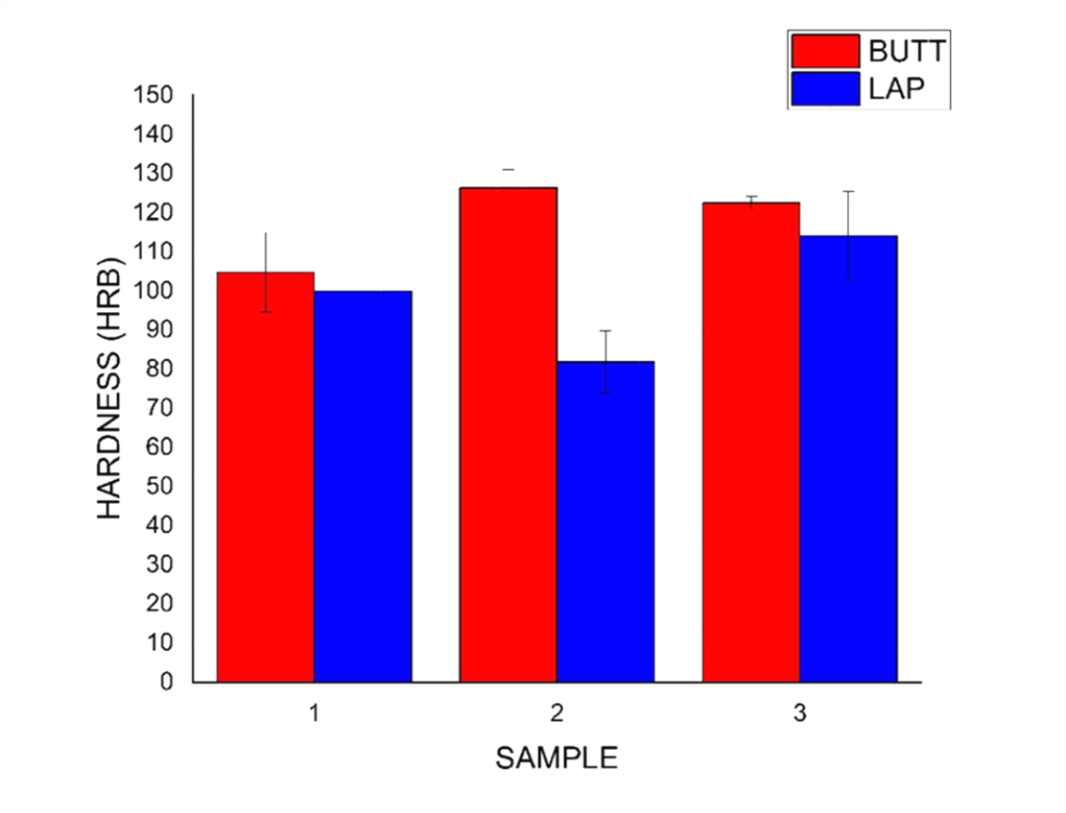

Figure 4.6: Hardness variation of the welded sample.

4.4 Tensile Test Results

The tensile test was conducted at Cape Coast Technical University's AVIC Civil Laboratory. The Universal Testing Machine WAW-1000H was the tensile test apparatus that was employed. While the test is being done, the device displays the test results on a computer

monitor. The length of the specimen was measured in relation to the change in applied force, which was the result of the tensile force employed to elongate the specimen. Three samples of each of the two welding types were utilized in the experiment.

4.4.1 Tensile Test Results for Butt and LAP Joint HAZ

The effects of heat input (current and welding speed) on the ultimate tensile strength of the weld heat-affected zone are shown in the **Figures 4.8**. A significant decrease in ultimate tensile strength value was recorded as the heat input increased which means the current increased and welding speed decreased or kept constant. Heat-affected zone tensile strength is lower than that of the parent metal by 18.5 %. The decrease in strength may be associated with the presence of void and other defects occurring because of increasing current. Excessive grain growth could also lead to a decrease in the tensile properties (Fekadu, 2018).

The results of the tensile test performed on the three-sample specimen each for the Butt and the LAP joints HAZ are shown in **Figures 4.8**. The findings show that under average stress of 23.1 MPa, LAP joints had an average ultimate tensile strength of 471.064 N/mm^2. With average stress of 24.3 MPa, the Butt joint also reported an average ultimate tensile strength of 496.0 N/mm^2. The graph of the LAP joint shows clearly that it has a very sharp yield point as compared to the Butt. This means that the welded Butt joint has slightly greater tensile strength and could bear much higher force than the welded LAP joint when the two welding techniques were compared using A36 mild steel with a 5mm thickness.

A

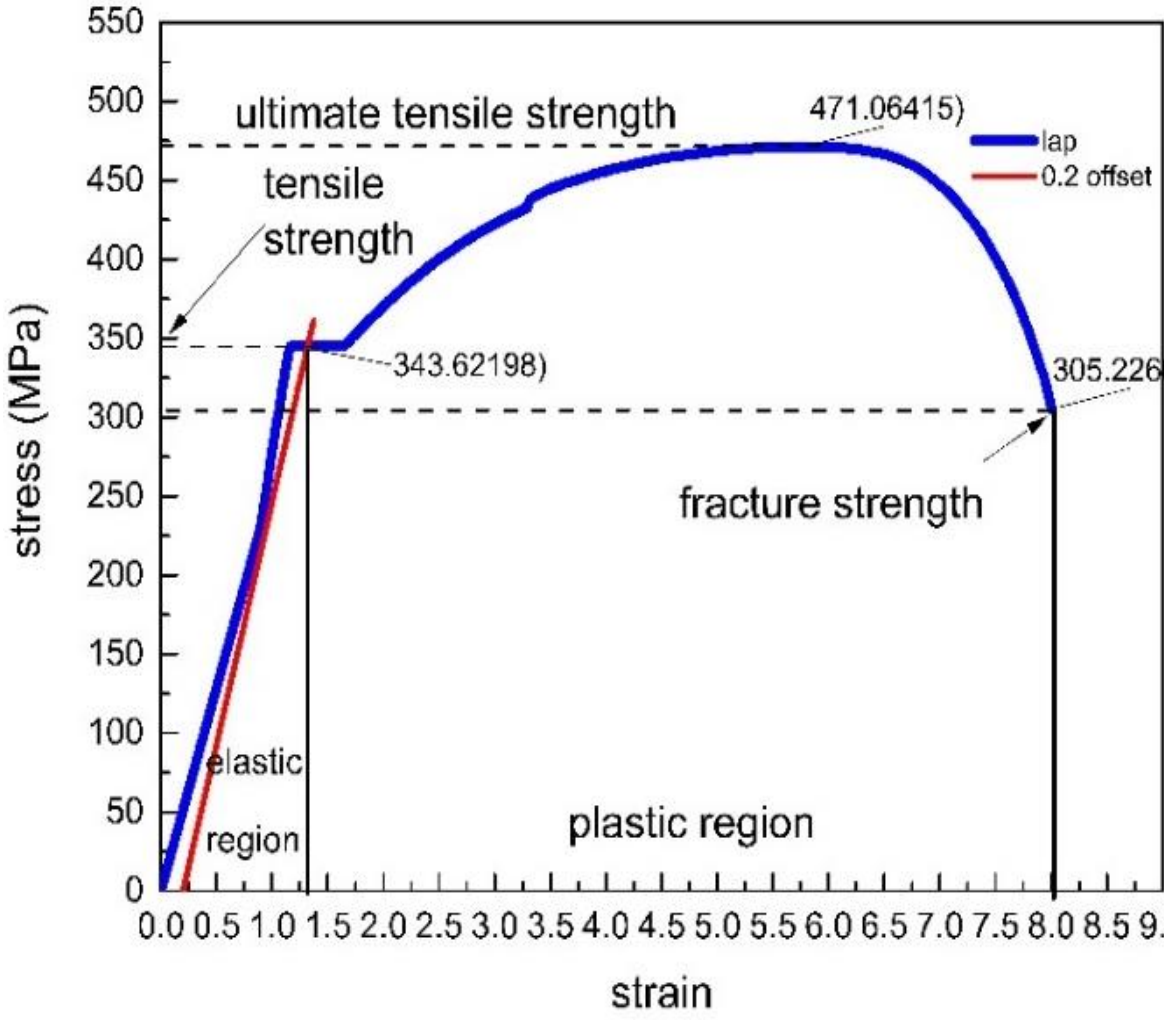
ultimate tensile strength
471.06415)
lap
0.2 offset
tensile
strength
343.62198)
305.226
fracture strength
elastic
region
plastic region
stress (MPa)
strain
550
500
450
400
350
300
250
200
150
100
50
0
0.0 0.5 1.0 1.5 2.0 2.5 3.0 3.5 4.0 4.5 5.0 5.5 6.0 6.5 7.0 7.5 8.0 8.5 9.

B

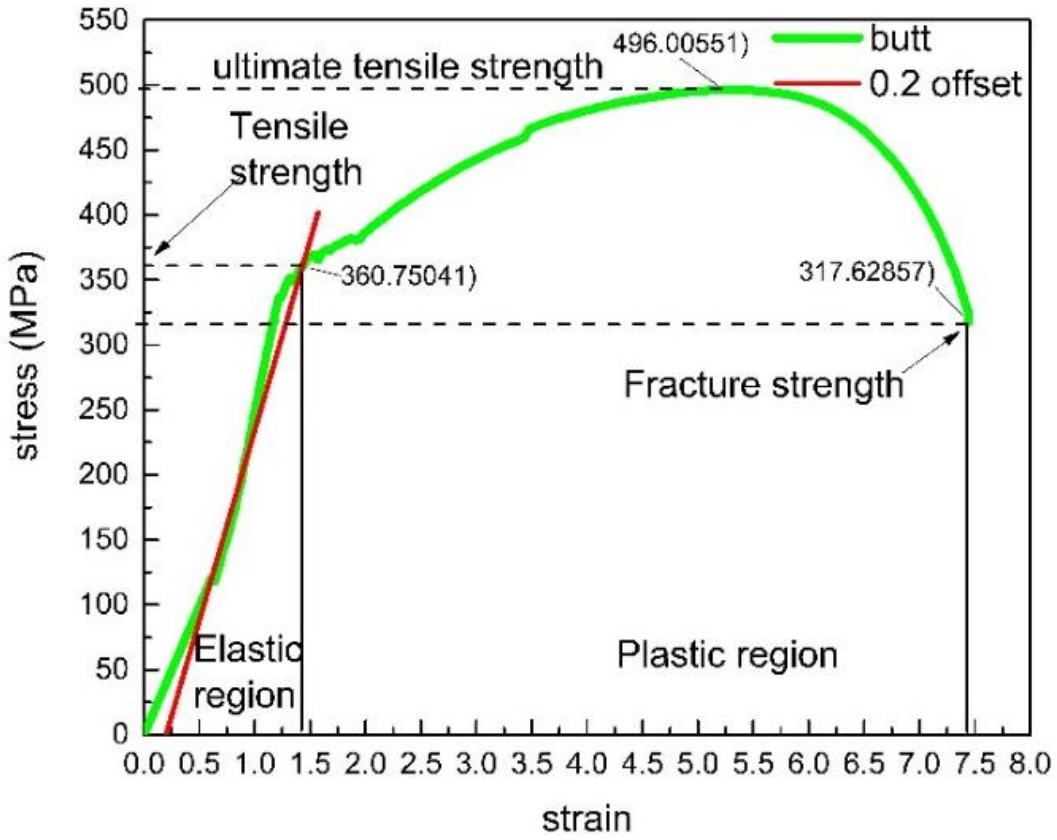

Figure 4.7: Stress-Strain curve of a) LAP b) Butt

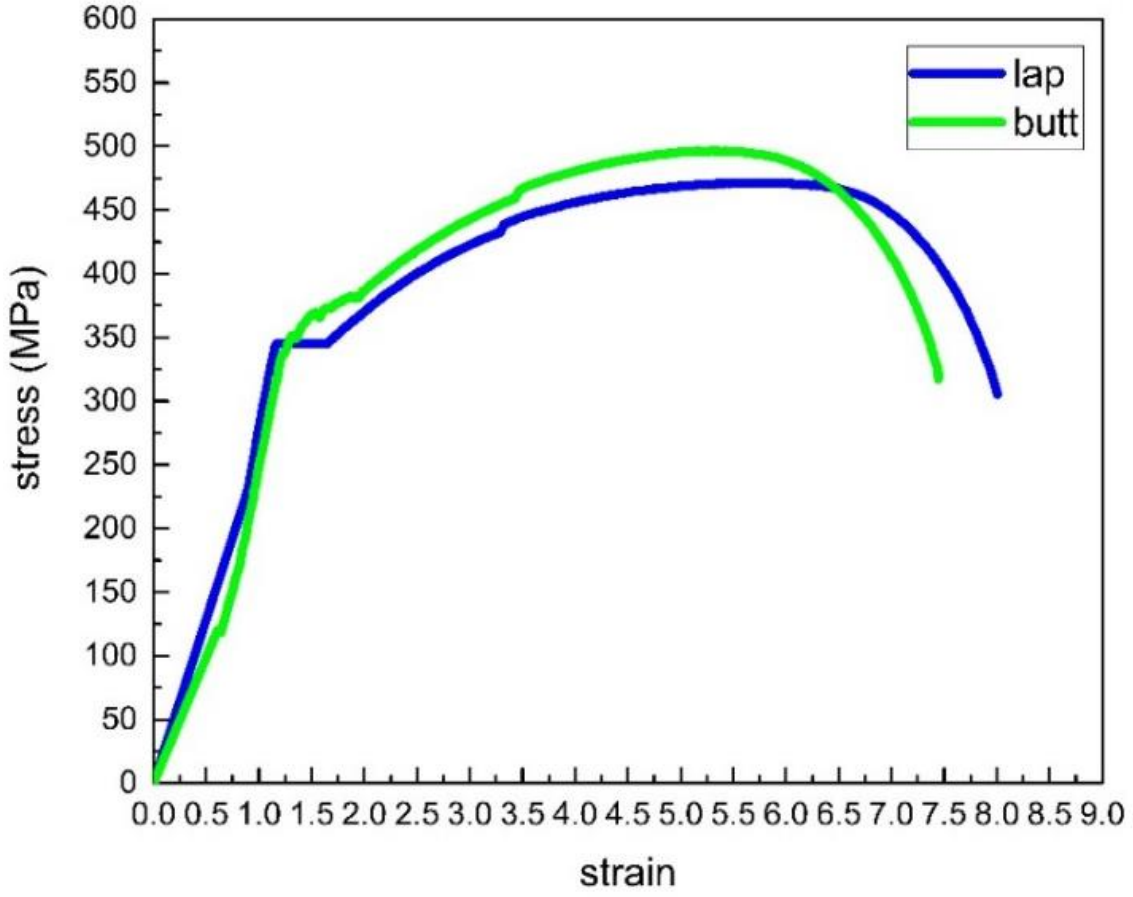

Figure 4.8 Stress-strain curve of a) LAP b) Butt and c) Butt and LAP welds.

Table 4.3: Comparing the tensile results of Butt and LAP HAZ.

PROPERTIES	**BUTT JOINT**	**LAP JOINT**
Yield stress (MPa)	360.75	343.62 MPa
Ultimate tensile stress (MPa)	496.00 MPa	471.00 MPa
Fracture stress (MPa)	317.62 MPa	305.00 MPa
Fracture strain	7.80	8.10
Young modules	292.73 MPa	307.905 MPa

4.4.2 Stress – Strain Analysis for Butt HAZ.

The results of the experimental setup for the tensile test are shown in the stress-strain analysis in Figure 4.7a. The elongation in the test specimens caused the plot to develop. The Butt joint's HAZ stress – strain curve as plotted shows that the Butt joint recorded maximum tensile stress of 496. MPa at a strain of 5.5. When the strain amounted to roughly 7.45 the material fails. According to the results, it is clear that the Butt-welded joint withstood larger stress, and thus, a less strain than the welded joint, which recorded a strain slightly higher than that of the Butt-welded HAZ joint.

4.4.3 Stress-Strain Analysis for LAP HAZ

Based on the results, it can be observed from the stress-strain curve in Fig. 4.9 that the LAP welded joint recorded the highest stress of 471 MPa at a strain of 8.1 in creating or establishing the association between the two. When the strain reached 5.3, there was a fracture. When the tension reached 8.1, the material broke down. With this setup, it is evident that when comparing the stress-strain of a LAP and Butt-welded joints HAZ, a LAP joint could not withstand much higher stress as compared with Butt welded joint.

CHAPTER FIVE

SUMMARY OF FINDINGS, CONCLUSION AND RECOMMENDATIONS

5.1 Introduction

This chapter focuses on the summary of findings, conclusion, and suggestions of the comparison of shielded metal arc Butt and LAP HAZ joint using A36 low carbon steel with a 5mm thickness.

5.2 Summary of Findings

This study looks into the microstructure surrounding the HAZ of A36 LCS and compares the results of tests for hardness, tensile strength, and microscopic analysis of A36 low carbon steel plate with a thickness of 5 mm that was welded using shielded metal arc welding (SMAW) to create butt and LAP joints. After being meticulously welded, the specimen was put through tensile tests on the WAW-1000B universal testing equipment. There were three test runs for every welded joint HAZ (Butt and LAP). An examination of the test data revealed that there was a noticeable decrease in the ultimate tensile strength value as the heat input increased. This happened as a result of higher welding current flowing at a steady or decreasing pace. The presence of flaws and voids. The experiment demonstrates that when heat input increases, the butt joint's heat-affected zone widens more than the LAP joint's. When examining the impact of welding speed and current on hardness, it is found that the former has a greater significance than the latter. In terms of the distributions of ferrites, pearlites, and other inclusions, the microstructure of each specimen in the heat-affected zone directly affects how hard the welded joint is.

The investigation's findings show that all of the Butt joints' heat affected zones (HAZs) had significant grain coarsening. Additionally, the extent of uniformly long dendritic grain in the HAZs increased with an increase in heat input, indicating that uniform solidification there occurred. In the LAP joint, elongated ferrite grains were visible in the shot of the region closest to the HAZ, which was caused by the direction of heat flow. At the fusing line, huge granules

have been seen pointing in the direction of a significant heat flow. Additionally, it is shown that there is no statistically significant variation in microstructure between the samples on the Butt and LAP tests.

5.3 Conclusions

In this study, the output data from mechanical tests conducted on the welded joints of 5 mm thick A36 mild steel plate were used to experimentally evaluate shielded metal arc welding techniques. The microstructure results demonstrate that uniform long dendrites and perlite in the Butt are signs of a uniform solidification process, whereas elongated ferrite grains in the LAP, which are apparent in the shot of the region nearest to the heat zone, are caused by the direction of heat flow. In this study, the output data from mechanical tests conducted on the welded joints of 5 mm thick A36 mild steel plate were used to experimentally evaluate shielded metal arc welding techniques. The microstructure results demonstrate that uniform long dendrites and perlite in the Butt are signs of a uniform solidification process, whereas elongated ferrite grains in the LAP, which are apparent in the shot of the region nearest to the heat zone, are caused by the direction of heat flow.

The experiment's hardness values for the LAP and Butt joints are As can be seen from the hardness value analysis, the Butt recorded a slightly higher hardness value for sample 1 (104.78 N/mm2) than the LAP (99.98 N/mm2). The hardness value for the LAP in the sample 2 joint HAZ was 81.82 N/mm2, and the hardness value for the Butt was 127.61 N/mm2. The sample 3 joint HAZ finally recorded the following values: 122.53 N/mw2 for the butt weld and 114.11 N/mm2 for LAP. It is clear from the numbers that, in addition to all the sample values displayed, the Butt registered a greater hardness value in all the test.

The results of the tensile test performed on the three-sample specimen each for the Butt and the LAP joints HAZ are shows under average stress of 23.1 MPa, LAP joints had an average ultimate tensile strength of 471.064 N/mm^2. With average stress of 24.3 MPa, the Butt joint

also reported an average ultimate tensile strength of 496.0 N/mm^2. The graph of the LAP joint shows clearly that it has a very sharp yield point as compared to the Butt. This means that the welded Butt joint has slightly greater tensile strength and could bear much higher force than the welded LAP joint when the two welding techniques were compared using A36 mild steel with a 5mm thickness.

A comparison of the mechanical properties of the HAZ of both joint types, indicates that the butt joint is the preferred choice when the area of application prioritizes hardness and strength. The Lap weld, however, has higher ductility, which renders its most suitable for application where toughness is a priority.

5.4 Recommendation

Using 5mm thick A36 low carbon steel plate to produce Butt and LAP joints, it is recommended to use the Butt junction instead of the LAP for analysing the mechanical qualities of a shielded metal arc welded joint based on the experimental results of this study. When comparing the tensile test of Butt and LAP welded joints when the linked work piece would or would be subjected to tensile test working settings, shielded metal arc Butt joints seem to be slightly more favourable than the others.

REFERENCE

Abioye, T. E. (n.d.). The effect of heat input on the mechanical and corrosion properties of AISI 304 electric arc weldments.

Ambade, S., Tembhurkar, C., Patil, A. P., Pantawane, P., & Singh, R. P. (2022a). Shielded metal arc welding of AISI 409M ferritic stainless steel: study on mechanical, intergranular corrosion properties and microstructure analysis. *World Journal of Engineering*, *19*(3), 266–273. https://doi.org/10.1108/WJE-03-2021-0146

Ambade, S., Tembhurkar, C., Patil, A. P., Pantawane, P., & Singh, R. P. (2022b). Shielded metal arc welding of AISI 409M ferritic stainless steel: study on mechanical, intergranular corrosion properties and microstructure analysis. *World Journal of Engineering*, *19*(3), 266–273. https://doi.org/10.1108/WJE-03-2021-0146

Anders, A. (2003). Tracking down the origin of arc plasma science I. Early pulsed and oscillating discharges. *IEEE Transactions on Plasma Science*, *31*(5 II), 1052–1059. https://doi.org/10.1109/TPS.2003.815476

Ashby, M. F. (1970). The deformation of plastically non-homogeneous materials. *Philosophical Magazine*, *21*(170), 399–424. https://doi.org/10.1080/14786437008238426

Assefa, A. T., Ahmed, G. M. S., Alamri, S., Edacherian, A., Jiru, M. G., Pandey, V., & Hossain, N. (2022). Experimental Investigation and Parametric Optimization of the Tungsten Inert Gas Welding Process Parameters of Dissimilar Metals. *Materials*, *15*(13). https://doi.org/10.3390/ma15134426

Chaudhary, V., Bharti, A., Azam, S. M., Kumar, N., & Saxena, K. K. (2021a). A re-investigation: Effect of TIG welding parameters on microstructure, mechanical, corrosion properties of welded joints. *Materials Today: Proceedings*, *45*, 4575–4580. https://doi.org/10.1016/j.matpr.2021.01.007

Chaudhary, V., Bharti, A., Azam, S. M., Kumar, N., & Saxena, K. K. (2021b). A re-investigation: Effect of TIG welding parameters on microstructure, mechanical, corrosion

properties of welded joints. *Materials Today: Proceedings*, *45*, 4575–4580. https://doi.org/10.1016/j.matpr.2021.01.007

Chaudhary, V., Bharti, A., Azam, S. M., Kumar, N., & Saxena, K. K. (2021c). A re-investigation: Effect of TIG welding parameters on microstructure, mechanical, corrosion properties of welded joints. *Materials Today: Proceedings*, *45*, 4575–4580. https://doi.org/10.1016/j.matpr.2021.01.007

Chaudhary, V., Bharti, A., Azam, S. M., Kumar, N., & Saxena, K. K. (2021d). A re-investigation: Effect of TIG welding parameters on microstructure, mechanical, corrosion properties of welded joints. *Materials Today: Proceedings*, *45*, 4575–4580. https://doi.org/10.1016/j.matpr.2021.01.007

Choi, I. C., Zhao, Y., Kim, Y. J., Yoo, B. G., Suh, J. Y., Ramamurty, U., & Jang, J. il. (2012). Indentation size effect and shear transformation zone size in a bulk metallic glass in two different structural states. *Acta Materialia*, *60*(19), 6862–6868. https://doi.org/10.1016/j.actamat.2012.08.061

Ghosh, N., Pal, P. K., & Nandi, G. (2016a). Parametric Optimization of MIG Welding on 316L Austenitic Stainless Steel by Grey-based Taguchi Method. *Procedia Technology*, *25*, 1038–1048. https://doi.org/10.1016/j.protcy.2016.08.204

Ghosh, N., Pal, P. K., & Nandi, G. (2016b). Parametric Optimization of MIG Welding on 316L Austenitic Stainless Steel by Grey-based Taguchi Method. *Procedia Technology*, *25*, 1038–1048. https://doi.org/10.1016/j.protcy.2016.08.204

Ghosh, N., Pal, P. K., & Nandi, G. (2016c). Parametric Optimization of MIG Welding on 316L Austenitic Stainless Steel by Grey-based Taguchi Method. *Procedia Technology*, *25*, 1038–1048. https://doi.org/10.1016/j.protcy.2016.08.204

Jeffus, L. F. (2004). *Welding principles and applications*. Thomson/Delmar Learning.

Jenney, C. L., O'Brien, A., American Welding Society, & Welding Handbook Committee. (2001). *Welding handbook*. American Welding Society.

Jenney, C. L., & O'brien Editors, A. (n.d.). *Welding Handbook Ninth Edition WELDING SCIENCE AND TECHNOLOGY Prepared under the direction of the Welding Handbook Committee*.

Joshi, J., & Thakkar, M. (2015). A Review on Parameters Optimization of Tungsten Inert Gas Welding using Taguchi's Design of Experiment Method. In *International Journal of Science and Research* (Vol. 6). www.ijsr.net

Kumar Yadav, P., Abbas, M., Patel, S., Author, C., & Kumar Yadav Praveen, P. (2014). ANALYSIS OF HEAT AFFECTED ZONE OF MILD STEEL SPECIMEN DEVELOPED DUE TO MIG WELDING. In *Int. J. Mech. Eng. & Rob. Res* (Vol. 3, Issue 3). www.ijmerr.com

Liu, F., Tan, C., Gong, X., Wu, L., Chen, B., Song, X., & Feng, J. (2020). A comparative study on microstructure and mechanical properties of HG785D steel joint produced by hybrid laser-MAG welding and laser welding. *Optics and Laser Technology*, *128*. https://doi.org/10.1016/j.optlastec.2020.106247

Malik Saadoon, A., Jha, R., & Jha, A. (2014). Influence of Welding Current and Joint Design on the Tensile Properties of SMAW Welded Mild Steel Joints Related papers A Review Paper on "Opt imizat ion of Shielded Metal Arc Welding Paramet ers for Welding of (M… Int ernat ional Journal of Scient ific Research in Science and Technology IJSRST Ut ilit y Fuzzy Taguchi Opt imizat ion Mult iple Qualit y Fact ors of Submerged Arc Welding.pdf Influence of Welding Current and Joint Design on the Tensile Properties of SMAW Welded Mild Steel Joints. In *Journal of Engineering Research and Applications www.ijera.com* (Vol. 4, Issue 6). www.ijera.com

Najafi, Y., Ghaini, F. M., Palizdar, Y., Shiri, S. G., & Pakniat, M. (2021). Microstructural characteristics of fusion zone in continuous wave fiber laser welded Nb-modified δ-TRIP steel. *Journal of Materials Research and Technology*, *15*, 3635–3646. https://doi.org/10.1016/j.jmrt.2021.09.116

Okelo Fekadu Advisor, B., Tilahun, D., Ababa, A., & Okelo Fekadu, B. (2018). *Investigation of Microstructure and Mechanical Properties of Heat Affected Zone in Manual Arc Welded Mild Steel A Thesis Submitted in Partial Fulfillment of the Requirements for the Degree of Master of Science in Mechanical Engineering (Mechanical Design Stream) SCHOOL OF MECHANICAL AND INDUSTRIAL ENGINEERING Investigation of Microstructure and Mechanical Properties of Heat Affected Zone in Manual Arc Welded Mild Steel MSc Thesis*.

Sakhawat, S., Falahati, A., Degischer, H. P., Spiradek, K., & Dománková, M. (2014). Localized ageing in the heat affected zone of welded X5CrNiCuNbl6-4 and X4CrNiSiTi14-7 sheets. *IOP Conference Series: Materials Science and Engineering*, *60*(1). https://doi.org/10.1088/1757-899X/60/1/012071

Shukla, A. A., Joshi, V. S., Chel, A., & Shukla, B. A. (2018a). Analysis of Shielded metal arc welding parameter on Depth of Penetration on AISI 1020 plates using Response surface methodology. *Procedia Manufacturing*, *20*, 239–246. https://doi.org/10.1016/j.promfg.2018.02.035

Shukla, A. A., Joshi, V. S., Chel, A., & Shukla, B. A. (2018b). Analysis of Shielded metal arc welding parameter on Depth of Penetration on AISI 1020 plates using Response surface methodology. *Procedia Manufacturing*, *20*, 239–246. https://doi.org/10.1016/j.promfg.2018.02.035

Singh, J., Kumar, G., & Garg, N. (2012). INFLUENCE OF VIBRATIONS IN ARC WELDING OVER MECHANICAL PROPERTIES AND MICROSTRUCTURE OF BUTT-WELDED-JOINTS. In *www.ijst.co.in* (Vol. 2, Issue 1). www.ijst.co.in

Singh, R. P., & Agrawal, M. K. (2021a). Influence of process parameters on depth of penetration of tungsten inert gas welded joints for low carbon steel AISI 1010 plates. *Materials Today: Proceedings*, *45*, 3656–3661. https://doi.org/10.1016/j.matpr.2021.01.032

Singh, R. P., & Agrawal, M. K. (2021b). Influence of process parameters on depth of penetration of tungsten inert gas welded joints for low carbon steel AISI 1010 plates. *Materials Today: Proceedings*, *45*, 3656–3661. https://doi.org/10.1016/j.matpr.2021.01.032

Singh, R. P., & Agrawal, M. K. (2021c). Influence of process parameters on depth of penetration of tungsten inert gas welded joints for low carbon steel AISI 1010 plates. *Materials Today: Proceedings*, *45*, 3656–3661. https://doi.org/10.1016/j.matpr.2021.01.032

Tadavi, T., Jogi, B., Dhende, S., Banait, S., & Wagh, P. (2017). *Microscopic Analysis of Heat Affected Zone (HAZ) of Submerged Arc Welding (saw) Joint for 1018 Mild Steel Sheet*. https://doi.org/10.2991/iccasp-16.2017.32

Wan, L., Huang, Y., Wang, Y., Lv, S., & Feng, J. (2015). Friction stir welding of aluminium hollow extrusion: Weld formation and mechanical properties. *Materials Science and Technology (United Kingdom)*, *31*(12), 1433–1442. https://doi.org/10.1179/1743284714Y.0000000721

Zhao, J., Wang, F., Huang, P., Lu, T. J., & Xu, K. W. (2014). Depth dependent strain rate sensitivity and inverse indentation size effect of hardness in body-centered cubic nanocrystalline metals. *Materials Science and Engineering A*, *615*, 87–91. https://doi.org/10.1016/j.msea.2014.07.057

Brykov, M. N., Petryshynets, I., Džupon, M., Kalinin, Y. A., Efremenko, V. G., Makarenko, N. A., Pimenov, D. Y. and Kováč, F. (2020) 'Microstructure and properties of heat affected zone in high-carbon steel after welding with fast cooling in water', *Materials*, 13(22), pp. 1–13. doi: 10.3390/ma13225059.

Fekadu, B. O. (2018) 'Investigation of Microstructure and Mechanical Properties of Heat Affected Zone in Manual Arc Welded Mild Steel A Thesis Submitted in Partial Fulfillment of the Requirements for the Degree of Master of Science in Mechanical Engineering'.

Laroui, W., Chegroune, R., Talaş, Ş., Keddam, M. and Badji, R. (2020) 'Microstructural and mechanical characterization of shielded metal arc welded dual phase steel joints', *Annales de Chimie: Science des Materiaux*, 44(6), pp. 381–386. doi: 10.18280/ACSM.440602.

Li, W., Cao, R., Zhu, W., Guo, X., Jiang, Y. and Chen, J. (2021) 'Microstructure evolution and impact toughness variation for high strength steel multi-pass weld metals with various cooling rates', *Journal of Manufacturing Processes*, 65, pp. 245–257. doi: 10.1016/J.JMAPRO.2021.03.027.

Pang, W., Ahmed, N. and Dunne, D. (2011) 'Low-Carbon Quenched and Tempered Steels'.

Parmar, A. and Dubey, A. (2017) 'Study of Heat Affected Zone for SMAW Process for Low Carbon Steel Specimen with controlled parameters', *International Journal of Modern Trends in Engineering & Research*, 4(11), pp. 23–28. doi: 10.21884/ijmter.2017.4339.cy2nc.

Węglowski, M. S., Zeman, M. and Grocholewski, A. (2016) 'Effect of welding thermal cycles on microstructure and mechanical properties of simulated heat affected zone for a We ldox 1300 ultra-high strength alloy steel', *Archives of Metallurgy and Materials*, 61(1), pp. 127–132. doi: 10.1515/amm-2016-0024.

Yadav, P. K., Abbas, M. and Patel, S. (2014) 'Analysis of Heat Affected Zone of Mild Steel', *International journal of mechanical engineering and Robotics Research*, 3(3), pp. 399–404. Available at: http://www.ijmerr.com/v3n3/ijmerr_v3n3_40.pdf.